Robust Ensemble Kalman Filter for Medium-Voltage Distribution System State Estimation

Manyun Huang, *Student Member, IEEE*, Zhinong Wei, *Member, IEEE*, Junbo Zhao, *Member, IEEE*, Rabih A. Jabr, *Fellow, IEEE*, Marco Pau, *Member, IEEE*, and Guoqiang Sun, *Member, IEEE*

***Abstract*— This article proposes a forecasting-aided medium-voltage (MV) distribution system state estimation (SE) method using a robust ensemble Kalman filter (REnKF). In the proposed solution, low-voltage (LV) measurements at the LV side of secondary substations are used together with the mathematical model of the MV/LV substations to derive new equivalent MV measurements. This yields the improvement of measurement redundancy and robustness of the REnKF to bad data and unknown system process noise. Specifically, we rely on the temporal correlations of the constructed innovation vector as well as the projection statistics (PS) to detect and modify the measurement error covariance matrix. Furthermore, the system process noise covariance matrix is updated adaptively to mitigate the impacts of uncertainties ON-state forecasting and measurement filtering. Extensive comparisons have been carried out with both the traditional EnKF and other SE formulations under balanced and unbalanced distribution system conditions. The results reveal that our proposed REnKF is able to obtain accurate SE results under various operation conditions, including the presence of intermittent renewable energy sources, bad data, and system unbalance.**

***Index Terms*— Adaptive system model, bad data, distribution system, ensemble Kalman filter (EnKF), robust estimation, state estimation (SE), low-voltage (LV) measurement.**

I. Introduction

RELIABLE and accurate nodal voltage magnitudes and angles play an important role in modern distribution system monitoring, optimization, and control [1]–[3]. State estimation (SE) is a fundamental tool employed in distribution management systems to identify the current operating states. A number of snapshot-based SE approaches have been proposed, including a single snapshot-based SE using the weighted least-squares (WLS) method [4]–[6] and multiple snapshots-based SE using Kalman filters [7]–[10].

The WLS has been widely used assuming that the measurement redundancy is high and the measurements are of good quality. However, this is difficult to achieve in practical distribution system [5]. To address the observability issue, pseudomeasurements were advocated [6]. The low precision of pseudomeasurements has, however, a significant impact on the accuracy of the distribution system SE results. In terms of forecasting-aided SE approaches, the challenge is how to model the state prediction model and perform the SE with a limited number of measurements [7]–[10]. In [7], a historical data-driven unscented Kalman filter (UKF) was proposed while in [8], the forecasted power injection measurements were used together with the particle filter for SE. However, these approaches still suffer from the limited accuracy of the available system measurements. Meanwhile, a sequential discrete Kalman filter [9] and an ensemble Kalman filter (EnKF) [10] were developed using measurements from the phasor measurement units (PMUs). However, they lack robustness to bad data and unknown system process noise.

The recent integration of smart meters and PMUs in modern electric power distribution systems allows the development of more advanced online load flow calculators and state estimators [11]–[16]. For example, the high-quality PMU measurements can be used with the traditional measurements for system monitoring [16]. In addition, there are some pilot projects for using pure PMU-based linear SE for distribution system, see [17]. However, the number of installed PMUs is usually insufficient for distribution system full observability due to communication infrastructure issues and economic reasons. By contrast, a large number of smart meters have been installed in low-voltage (LV) distribution systems worldwide [18]. To this end, some studies have exploited the smart meter data of the LV distribution systems to improve SE performance. For example, Al-Wakeel *et al*. [19] proposed to extract information from both historical and real-time smart meters for the medium-voltage (MV)

Manuscript received June 27, 2019; revised August 18, 2019; accepted September 28, 2019. Date of publication October 10, 2019; date of current version June 9, 2020. This work was supported by the National Key Research and Development Program of China under Grant 2018YFB0904500, and in part by the University Graduate Research and Innovation Projects of Jiangsu Province under Grant KYCX18_0545. The Associate Editor coordinating the review process was Dr. Carlo Muscas. *(Corresponding author: Manyun Huang.)*

M. Huang, Z. Wei, and G. Sun are with the College of Energy and Electrical Engineering, Hohai University, Nanjing 210098, China (e-mail: hmy_hhu@yeah.net; wzn_nj@263.net; hhusunguoqiang@163.com).

J. Zhao is with the Department of Electrical and Computer Engineering, Mississippi State University, Starkville, MS 39759 USA (e-mail:junbo@ece.msstate.edu).

R. A. Jabr is with the Department of Electrical and Computer Engineering, American University of Beirut, Beirut 1107 2020, Lebanon (e-mail: rabih.jabr@aub.edu.lb).

M. Pau is with the Institute for Automation of Complex Power Systems, RWTH Aachen University, 52062 Aachen, Germany (e-mail: mpau@eonerc.rwth-aachen.de).

Color versions of one or more of the figures in this article are available online at http://ieeexplore.ieee.org.

Digital Object Identifier 10.1109/TIM.2019.2945743

distribution system SE using an iteratively reweighted least-squares state estimator. Chen *et al.* [20] investigated the impact of smart meter data aggregation on the SE of MV distribution systems. Liao *et al.* [21] used historical smart meter data to estimate the topology of distribution systems. However, the data quality issues associated with smart meters have not been addressed and there is still a grand challenge of how to combine smart meter and traditional measurements effectively for improving SE accuracy. Furthermore, the inherent temporal correlations among the nodal voltage magnitudes and angles have not been thoroughly considered to enhance the distribution system measurement redundancy.

To address these challenges, this article proposes a forecasting-aided MV distribution system SE method. It yields the following contributions.

1) The robust ensemble Kalman filter (REnKF) is first developed to deal with bad data and further extended to integrate the adaptive process noise covariance matrix to mitigate the impacts of uncertainties on state forecasting and state filtering.
2) Instead of relying on low-precision pseudomeasurements for improving the measurement redundancy, we propose to extend the approaches in [11] and [22] for distribution system SE, where smart meter measurements taken at the LV side of secondary substations are used together with the mathematical model of the MV/LV substation to derive new equivalent MV measurements. These derived power measurements from these smart meters have higher accuracy than the pseudomeasurements from short-term load or renewable energy power forecasts. They are also cheaper than installing new measurement instruments at the MV system [22].
3) We show that the consideration of temporal correlations among the nodal voltage magnitudes and angles enables more accurate state estimates and better robustness against bad data. Specifically, we rely on the temporal correlations of the constructed innovation vector as well as the projection statistics (PS) to detect bad data and modify the measurement error covariance matrix. We also show that due to the use of pseudomeasurements with large uncertainties, the normalized residual (NR) statistical test may fail to work in the distribution system SE.
4) Extensive comparisons have been carried out with other SE alternatives under balanced and unbalanced MV distribution systems. The results reveal that our proposed REnKF is able to obtain accurate SE results under various operation conditions. It also validates the benefits of installing smart meter devices at the LV side of the MV/LV substations.

The remainder of this article is organized as follows: Section II describes the distribution system SE problem formulation, including the conventional static SE and the forecasting-aided SE. In Section III, the proposed REnKF framework is presented. The results are shown in Section IV to demonstrate the effectiveness and robustness of the proposed REnKF, and finally, Section V concludes this article.

II. Distribution State Estimation Problem Formulation

We first describe the formulation of conventional static SE using WLS. Then, its associated challenges are discussed, followed by the development of forecasting-aided SE considering the model of the MV/LV substation.

A. Conventional Static SE Formulation

The general measurement model for distribution systems can be expressed as follows:

$$\mathbf{z} = h(\mathbf{x}) + \mathbf{v} \tag{1}$$

where $\mathbf{x}$ is a $2n \times 1$ system state vector, i.e., voltage magnitudes and angles of n nodes, $\mathbf{z}$ is a $m \times 1$ measurement vector, $h(\cdot)$ represents the vector of measurement functions, and $\mathbf{v}$ is a $m \times 1$ measurement noise vector; it is usually assumed to be Gaussian white noise with covariance matrix $\mathbf{R} = \text{diag}\{\sigma_1^2, \sigma_2^2, \ldots, \sigma_m^2\}$, where σ_i is the standard deviation of the ith measurement error.

In the WLS method, the normal equations are used to find the iteration solution as shown in the following equation:

$$[\mathbf{G}(\mathbf{x}^j)]\Delta\mathbf{x}^{j+1} = \mathbf{H}^T(\mathbf{x}^j)\mathbf{R}^{-1}[\mathbf{z} - h(\mathbf{x}^j)] \tag{2}$$

where $\Delta\mathbf{x}^{j+1} = \mathbf{x}^{j+1} - \mathbf{x}^j$ is the update of the system state vector at iteration j, $\mathbf{H}^{\mathrm{T}}(\mathbf{x}^j) = \partial h(\mathbf{x}^j)/\partial \mathbf{x}^j$ is a $m \times 2n$ measurement Jacobian matrix, and $\mathbf{G}(\mathbf{x}^j) = \mathbf{H}^{\mathrm{T}}(\mathbf{x}^j)\mathbf{R}^{-1}\mathbf{H}(\mathbf{x}^j)$ is a $2n \times 2n$ gain matrix. The final solution is obtained when the absolute value of $\Delta\mathbf{x}^{j+1}$ is smaller than a preset threshold.

Due to the limited number of real-time measurements in the distribution system, pseudomeasurements are typically added to increase the measurement redundancy. However, their weights are challenging to tune in practice. When moving to the lower voltage levels of the electrical system, it becomes more and more difficult to obtain accurate forecasts for the pseudomeasurement (due to the larger role played by the random behavior of single customers) and this automatically affects the accuracy of the achievable predictions. Therefore, very large uncertainties have to be used for those pseudomeasurements, which in the end degrade also the accuracy of the state estimator. To address this issue, a forecasting-aided SE based on LV smart meter measurements is advocated and discussed in Section II-B.

B. Forecasting-Aided SE Formulation

The general form of a forecasting-aided SE for distribution systems can be written as follows:

$$\mathbf{x}_k = f(\mathbf{x}_{k-1}) + \mathbf{w}_k \tag{3}$$

$$\mathbf{z}_k = h(\mathbf{x}_k) + \mathbf{v}_k \tag{4}$$

where $\mathbf{x}_k = [V_{1,k}V_{2,k}\ldots V_{n,k}\boldsymbol{\theta}_{1,k}\boldsymbol{\theta}_{2,k}\ldots\boldsymbol{\theta}_{n,k}]^{\mathrm{T}}$ is the state vector consisting of nodal voltage magnitudes and angles,

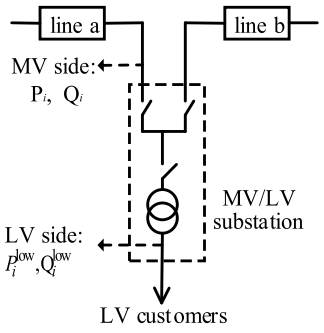

Fig. 1. Schematic illustrating the MV/LV substation model.

$\mathbf{z}_k = [z_{1,k} z_{2,k} \ldots z_{m,k}]^{\mathrm{T}}$ is the measurement vector, $f(\cdot)$ represents the state transition function relating $\mathbf{x}_k$ to $\mathbf{x}_{k-1}$, and $\mathbf{w}_k$ and $\mathbf{v}_k$ represent system process noise and measurement noise, respectively. They are assumed to be with zero means and covariance matrices $\mathbf{Q}_k$ and $\mathbf{R}_k$, respectively. The forecasting-aided SE involves a forecast and a filtering procedure to track the stochastic variations of distribution system state variables.

Problem Statement: The pseudomeasurements are usually required for distribution system observability, and the precision of pseudomeasurements limits the estimation accuracy. Instead of leveraging pseudomeasurements, we propose to derive measurements from smart meters that are installed mainly at the LV side of MV/LV substations [11], [22]. Note that such smart meter installation is being promoted in cities of China and, in the simulations, a realistic example of a distribution network with this measurement configuration will be considered. In particular, we treat each MV/LV substation as a node of the MV network as illustrated in Fig. 1. As the LV side of the substation is usually measured by a smart meter, equivalent active and reactive load powers at the MV side of the node have to be derived. It should be noted that the derived power measurements from smart meters have higher accuracy than the pseudomeasurements from load or renewable energy power injection forecasts. In addition, thanks to the widespread installation of smart meter devices, a large number of such derived equivalent power measurements can be obtained, yielding a significantly improved measurement redundancy. This allows us to improve estimation accuracy as well as design robust estimators against bad data.

To be specific, it can be seen from Fig. 1 that the equivalent active and reactive load powers at the MV side of node i ($P_{i,k}$ and $Q_{i,k}$) at time k can be calculated via the formula from [11] and [22]

$$P_{i,k} = P_{i,k}^{\mathrm{low}} + P_{\mathrm{no},i} + P_{\mathrm{short},i}\left(\left|S_{i,k}^{\mathrm{low}}\right|/S_{\mathrm{rate},i}\right)^2 \tag{5}$$

$$Q_{i,k} = Q_{i,k}^{\mathrm{low}} + Q_{\mathrm{no},i} + Q_{\mathrm{short},i}\left(\left|S_{i,k}^{\mathrm{low}}\right|/S_{\mathrm{rate},i}\right)^2 \tag{6}$$

where $S_{i,k}^{\mathrm{low}} = P_{i,k}^{\mathrm{low}} + jQ_{i,k}^{\mathrm{low}}$ is the real-time complex load power of LV customers measured by smart meter, $P_{\mathrm{no},i}$ and $Q_{\mathrm{no},i}$ are the no-load active and reactive power losses, respectively, $P_{\mathrm{short},i}$ and $Q_{\mathrm{short},i}$ are the short-circuit active and reactive power losses, respectively, and $S_{\mathrm{rate},i}$ is the rated apparent power of the MV/LV substation at node i. The standard deviation of the derived equivalent power measurements ($\sigma_{\mathrm{P}i,k}$ and $\sigma_{\mathrm{Q}i,k}$) can be obtained according to the measurement uncertainty propagation rules, yielding

$$\sigma_{P_{i,k}}^2 = \left(\frac{\partial P_{i,k}}{\partial P_{i,k}^{\mathrm{low}}}\right)^2 \sigma_{P_{i,k}^{\mathrm{low}}}^2 + \left(\frac{\partial P_{i,k}}{\partial Q_{i,k}^{\mathrm{low}}}\right)^2 \sigma_{Q_{i,k}^{\mathrm{low}}}^2 \tag{7}$$

$$\sigma_{Q_{i,k}}^2 = \left(\frac{\partial Q_{i,k}}{\partial P_{i,k}^{\mathrm{low}}}\right)^2 \sigma_{P_{i,k}^{\mathrm{low}}}^2 + \left(\frac{\partial Q_{i,k}}{\partial Q_{i,k}^{\mathrm{low}}}\right)^2 \sigma_{Q_{i,k}^{\mathrm{low}}}^2 \tag{8}$$

where $\sigma_{Pi,k}^{\mathrm{low}}$ and $\sigma_{Qi,k}^{\mathrm{low}}$ are the standard deviations of the real-time power measurements at the LV side obtained by the smart meters; they are derived from the data sheets of the smart meter devices provided by the corresponding manufacturer.

In this article, the formulations of (5) and (6) are used to derive equivalent active and reactive power injections with the assumption that smart meter data are available at the LV side. Note that the MV/LV substation model described in (5) and (6) is built for three-phase balanced distribution systems. In unbalanced conditions, the real-time load powers at the LV side are obtained from the three phases, i.e., $\{P_{i,k}^{\mathrm{low}}, Q_{i,k}^{\mathrm{low}}\}_{\mathrm{a,b,c}}$, and the aforementioned formulations work fine for the transformer with the same connection at the MV and LV sides (e.g., star to star). If there are other transformer connections, e.g., delta to star, the three-phase transformer model can be built as the equivalent admittance matrix and core loss block by the approach in [23].

To solve the above forecasting-aided SE problem, the well-known extended Kalman filter (EKF) can be used. Specifically, the EKF relies on the first-order Taylor series expansion, which may yield unreliable results in the presence of strong system nonlinearity. To address this issue, the UKF that approximates the mean and covariance via the unscented transformation is advocated. Both approaches have recently been applied to power systems in [24] and [25], respectively. To achieve a better estimation accuracy for the nonlinear system having strong nonlinearity, the EnKF has been developed in [10] and [26] at the expense of additional computational efforts. As the distribution system model is nonlinear, a REnKF that has the capability of dealing with bad data and unknown system process noises is developed next.

III. Proposed Robust Ensemble Kalman Filter

The proposed REnKF includes four main procedures: state forecasting, measurement filtering, erroneous measurements data detection, as well as state forecasting model adjustment. They are described in detail below. Note that, to the best of authors' knowledge, this is the first time that the REnKF is developed for power system distribution system SE.

In the following, all the procedures for the REnKF are presented for an equivalent single-phase model of the grid. In the distribution system, however, unbalanced conditions commonly occur, and this calls for the development of a three-phase model. The presented procedure for the REnKF can be easily adapted to the three-phase scenario, and the state vector $\boldsymbol{x}$ becomes a $6n \times 1$ vector composed of the three-phase voltage magnitudes and angles of the n nodes, and the measurement vector $\boldsymbol{z}$ consists of m multiphase measurements (i.e., for each

measurement point the meter provides the per-phase values of the measured quantities). The resulting measurement function vector $h(\cdot)$ for the three-phase model can be found in [27].

A. Ensemble Kalman Filter

The conventional EnKF employs a collection of state vectors, named an ensemble, to solve a recursive filter problem [10], [26]. In the first step, the distribution system states at time k are processed with the EnKF, which provides two functionalities: state forecasting and measurement filtering. Given the estimated state vector $\hat{\mathbf{x}}_{k-1}$ and its covariance matrix $\mathbf{P}_{k-1}$ at time $k-1$, the ensemble of forecasted states $\{\hat{\mathbf{x}}^i_{k|k-1}\}^q_{i=1}$ at time k can be expressed as follows:

$$\hat{\mathbf{x}}^i_{k|k-1} = \hat{\mathbf{x}}^i_{k-1} + \mathbf{w}^i_k \tag{9}$$

where q is the chosen number of ensembles and superscript i indicates the ith ensemble. Then, the forecasted states $\hat{\mathbf{x}}_{k|k-1}$ and their covariance matrix $\mathbf{P}_{k|k-1}$ can be derived as follows:

$$\hat{\mathbf{x}}_{k|k-1} = \frac{1}{q}\sum_{i=1}^{q}\hat{\mathbf{x}}^i_{k|k-1} \tag{10}$$

$$\mathbf{P}_{k|k-1} = \frac{1}{q-1}\sum_{i=1}^{q}\left(\hat{\mathbf{x}}^i_{k|k-1} - \hat{\mathbf{x}}_{k|k-1}\right)\left(\hat{\mathbf{x}}^i_{k|k-1} - \hat{\mathbf{x}}_{k|k-1}\right)^T. \tag{11}$$

After state predictions, the ensembles of the prediction measurements $\{\hat{\mathbf{z}}^i_{k|k-1}\}^q_{i=1}$ can be evaluated at $\hat{\mathbf{x}}^i_{k|k-1}$ based on the following nonlinear measurement function:

$$\hat{\mathbf{z}}^i_{k|k-1} = h\left(\hat{\mathbf{x}}^i_{k|k-1}\right) \tag{12}$$

$$\hat{\mathbf{z}}_{k|k-1} = \frac{1}{q}\sum_{i=1}^{q}\hat{\mathbf{z}}^i_{k|k-1} \tag{13}$$

$$\mathbf{P}^{xz}_{k|k-1} = \frac{1}{q-1}\sum_{i=1}^{q}\left(\hat{\mathbf{x}}^i_{k|k-1} - \hat{\mathbf{x}}_{k|k-1}\right)\left(\hat{\mathbf{z}}^i_{k|k-1} - \hat{\mathbf{z}}_{k|k-1}\right)^T \tag{14}$$

$$\mathbf{P}^{zz}_{k|k-1} = \frac{1}{q-1}\sum_{i=1}^{q}\left(\hat{\mathbf{z}}^i_{k|k-1} - \hat{\mathbf{z}}_{k|k-1}\right)\left(\hat{\mathbf{z}}^i_{k|k-1} - \hat{\mathbf{z}}_{k|k-1}\right)^T + \mathbf{R}_k \tag{15}$$

$$\mathbf{K}_k = \mathbf{P}^{xz}_{k|k-1}\left(\mathbf{P}^{zz}_{k|k-1}\right)^{-1} \tag{16}$$

where $\hat{\mathbf{z}}_{k|k-1}$ is the predicted measurement vector and $\mathbf{K}_k$ is a $2n \times m$ gain matrix calculated by the covariance matrices $\mathbf{P}^{xz}_{k|k-1}$ and $\mathbf{P}^{zz}_{k|k-1}$. Finally, the measurement vector $\mathbf{z}_k$ is used together with the forecasted information to get the filtered states as follows:

$$\hat{\mathbf{x}}^i_k = \hat{\mathbf{x}}^i_{k|k-1} + \mathbf{K}_k\left(\mathbf{z}_k - \hat{\mathbf{z}}^i_{k|k-1}\right) \tag{17}$$

$$\hat{\mathbf{x}}_k = \frac{1}{q}\sum_{i=1}^{q}\hat{\mathbf{x}}^i_k \tag{18}$$

$$\mathbf{P}_k = \frac{1}{q-1}\sum_{i=1}^{q}\left(\hat{\mathbf{x}}^i_k - \hat{\mathbf{x}}_k\right)\left(\hat{\mathbf{x}}^i_k - \hat{\mathbf{x}}_k\right)^T \tag{19}$$

where $\hat{\mathbf{x}}_k$ is the estimated state vector at time k with its covariance matrix $\mathbf{P}_k$.

B. Bad Data Detection and Measurement Error Covariance Matrix Modification

In the aforementioned measurement filtering stage, the probability distribution of $\mathbf{v}_k$ is assumed to be a Gaussian distribution with variance matrix $\mathbf{R}_k = \text{diag}\{\sigma_{1,k}{}^2, \sigma_{2,k}{}^2, \ldots, \sigma_{m,k}{}^2\}$, where $\sigma_{i,k}$ is the standard deviation of measurement $z_{i,k}$. In practice, the received measurements in a distribution system may be biased due to a number of reasons, such as communication noise, measurement device deviation, and gross measurement errors. As a result, the measurement uncertainty assumptions no longer hold, yielding biased state estimates. To address that, we propose to leverage PS for the identification of bad measurements and then modify the measurement error covariance matrix accordingly.

As discussed in Section II-A, the distribution system states vary according to the changes in the load and renewable energy injections. The latter is dependent heavily on weather conditions and show strong correlations in similar geographic areas. Therefore, there exist correlations between the forecasted and received online measurements. In other words, the measurement innovation vectors should be consistent in the absence of bad data. Motivated by this, we propose to apply the PS to the following matrix $\mathbf{M}_k$ for bad data detection:

$$\mathbf{M}_k = [\mathbf{z}_k - \hat{\mathbf{z}}_{k|k-1}, \mathbf{z}_{k-1} - \hat{\mathbf{z}}_{k-1|k-2}] \tag{20}$$

where $\mathbf{z}_k - \hat{\mathbf{z}}_{k|k-1}$ and $\mathbf{z}_{k-1} - \hat{\mathbf{z}}_{k-1|k-2}$ are the innovation vectors at time k and $k-1$, respectively. Then, a measurement $z_{i,k}$ is declared to be erroneous if

$$PS_{i,k} > b_i \tag{21}$$

where $PS_{i,k}$ is the PS value associated with measurement $z_{i,k}$. The mathematical expression of how PS values are calculated can be found in [28]. The detection threshold b_i of $z_{i,k}$ is set to be $\chi^2_{2,0.975}$ as the PS values follow a chi-squared distribution with two degrees of freedom. To reduce the negative impact of outliers on the estimation results, the standard deviation of an identified outlier $z_{i,k}$ is modified as

$$\sigma^2_{i,k} = \max\{1, (PS_{i,k}/d_i)^2\} \tag{22}$$

where parameter d_i is set to 1.5 and the modified $\sigma^2_{i,k}$ is employed to obtain a new measurement error covariance matrix $\mathbf{R}_k$. The measurement filtering is then conducted again with the revised $\mathbf{R}_k$ to obtain the final estimation results.

C. State Forecasting Model Adjustment

Similar to the measurement noise assumption, the system process noise $\mathbf{w}_k$ is normally assumed to be white Gaussian with covariance matrix $\mathbf{Q}_k$. Note that $\mathbf{Q}_k$ is generally assumed to be a constant [8]–[10]. However, as the system operating conditions vary continously, the identified state transition model may induce biases if they are kept constant. In fact, the system process noise should be updated from time to time to compensate for the model inadequacy. Motivated by that this article proposes to adopt a signal processing technique [29] for system process noise covariance matrix updating. Note that the application of [29] for power system estimation has not been done before. Our efforts lie in integrating this technique to

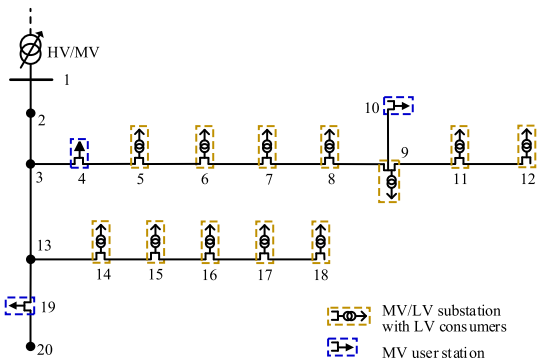

Fig. 2. Actual MV distribution system in China.

the developed REnKF framework with more adaptiveness of dealing with unknown system process noise. Specifically, let us define the deviation between the forecasted states and the estimation states as follows:

$$\xi_k = \hat{x}_k - \hat{x}_{k|k-1} \tag{23}$$

where $\boldsymbol{\xi}_k$ is a $2n \times 1$ forecasted deviation vector at time k. Then, for a given time horizon T, the relationship between $\boldsymbol{\xi}_k$ and the covariance matrix of $\mathbf{w}_k$ is shown in the following equation:

$$\bar{\xi}_k = \frac{T-1}{T}\bar{\xi}_{k-1} + \frac{1}{T}\xi_k \tag{24}$$

$$\Delta\mathbf{Q}_k = \frac{1}{T-1}(\xi_k - \bar{\xi}_k)(\xi_k - \bar{\xi}_k)^T - \frac{1}{T}(\mathbf{P}_{k|k-1} - \mathbf{Q}_{k-1} - \mathbf{P}_k) \tag{25}$$

$$\mathbf{Q}_k = \frac{T-1}{T}\mathbf{Q}_{k-1} + \Delta\mathbf{Q}_k. \tag{26}$$

Here, $\bar{\boldsymbol{\xi}}_k$ is the mean value of $\boldsymbol{\xi}_i$ from $k-T+1$ to k, and $\Delta\mathbf{Q}_k$ is the correction term of $\mathbf{Q}_k$. The benefits of updating $\mathbf{Q}_k$ include the tracking of system states continuously as well as improved forecasting capability of the states at the next time.

IV. Simulation and Results

In this section, the proposed REnKF is first tested in an actual MV distribution system located at Jiangsu province in China. The selected MV distribution system is displayed in Fig. 2, where smart meters are installed at the LV side of each MV/LV substation. It is composed of a main substation with an HV/MV transformer, 20 nodes and 19 branches with three MV user stations and 12 MV/LV substations with LV consumers. The parameters of all branches and MV/LV transformers are given in the Appendix. In the simulations, the system states are updated every 15 min for 24 h (96 time instants) via the distribution system SE, since the refresh rate of the LV smart meter data for the actual grid is expected to be 15 min. All simulations were performed on a PC with an Intel Core i5-5200U CPU, 8 GB of RAM, and the calculations are conducted in a MATLAB R2014a environment. The reference operating conditions of the distribution system are obtained from the load flow calculations based on the Newton–Raphson method.

Specifically, the conventional measurements at the MV system are the voltage magnitude measurements of node 1, the power injection measurements of nodes 4, 10, and 19, and the power flow measurements of branches 1-2, 3-4, and 13-14. The LV measurements derived from the smart meters in the proposed approach are the load active and reactive power measurements provided at the LV side of each MV/LV substation (nodes 5, 6, 7, 8, 9, 11, 12, 14, 15, 16, 17, and 18). It is worth noting that different measurement technologies, like those employed at the MV and the LV level, could be characterized by different reporting rates. In this case, the meters with the slowest refresh rate are the bottleneck for the reporting rate of the SE algorithm itself. Moreover, time synchronization issues could also arise. Time synchronization should be possibly ensured among the meters to guarantee the collection of measurement data referred to the same instant of time. This can be potentially obtained (with different levels of synchronization accuracy) using dedicated synchronization protocols, like the Precision Time Protocol (PTP) [30]. When the time synchronization cannot be guaranteed, instead, ad hoc solutions like the one proposed in [31] can be implemented to consider the additional uncertainty brought by the time delays.

The MV and LV measurements used in the simulations were considered as synchronized, and they were corrupted by adding random noises to simulate only the measurement uncertainties arising due to the accuracy of the components in the measurement chain (sensors and measurement devices). For MV measurements, the added noise of voltage magnitude measurements was assumed to be Gaussian white noise with a 0.5% accuracy level, while those of the power injection and power flow measurements were assumed to be Gaussian white noise with a 1% accuracy level (as in [32]). The added noise of the LV measurements was assumed to be Gaussian white noise with a 3% accuracy level (as in [33]). In addition, the zero injection powers of nodes 2, 3, 13, and 20 were taken into consideration (with large weights, as they are perfect measurements). Pseudomeasurements obtained through short-term load forecasting are usually used by distribution system SE, and they have much lower accuracy than the real-time measurements [6], [13]. In this article, they are used for performance comparison purposes and it is assumed that their errors follow Gaussian probability distributions with 30% standard deviations.

As the main term of comparison, two other methods were tested, namely: 1) traditional WLS: only MV measurements, the zero injections, and pseudomeasurements of LV load powers are used. In addition, the NR statistical test was used to detect bad data and 2) traditional EnKF: employs the same measurement set as the traditional WLS. The initial conditions of EnKF and REnKF are defined as follows: $\mathbf{x}_0$ is set based on load flow calculations; the diagonal elements of $\mathbf{P}_0$ are 10^{-6}, and q is 600 so as to achieve a good tradeoff between computational speed and accuracy [10]. T parameter of the REnKF is set to be 50 time instants based on the assumption that the covariance of $\mathbf{w}_k$ changes slowly in this time horizon. The latter usually holds true in practice as the process noise statistics do not change frequently. Note that T can be tuned in advance via offline tests under different scenarios.

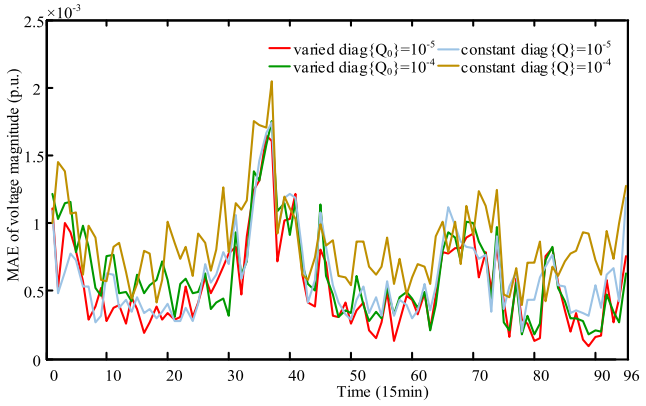

Fig. 3. MAE of node voltage magnitudes for the forecasted states by the proposed REnKF with different values of diag{$\mathbf{Q}_0$} or diag{$\mathbf{Q}$}.

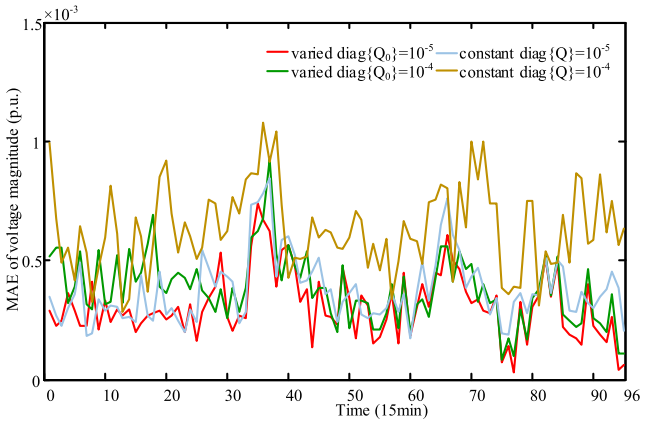

Fig. 4. MAE of node voltage magnitudes for the state estimates by the proposed REnKF with different values of diag{$\mathbf{Q}_0$} or diag{$\mathbf{Q}$}.

The performances of these methods are, respectively, evaluated in terms of nodal voltage magnitude and the voltage angle based on the mean absolute error (MAE) [34]

$$\mathrm{MAE}_k^V = \frac{1}{2n}\sum_{i=1}^{2n}\left|\hat{V}_{i,k}^{\mathrm{est}} - V_{i,k}^{\mathrm{true}}\right| \tag{27}$$

$$\mathrm{MAE}_k^\theta = \frac{1}{2n}\sum_{i=1}^{2n}\left|\hat{\theta}_{i,k}^{\mathrm{est}} - \theta_{i,k}^{\mathrm{true}}\right| \tag{28}$$

where $\hat{V}_{i,k}^{\mathrm{est}}$ and $V_{i,k}^{\mathrm{true}}$ are, respectively, the estimated and true voltage magnitudes of node i, and $\hat{\theta}_{i,k}^{\mathrm{est}}$ and $\theta_{i,k}^{\mathrm{true}}$ are the estimated and true voltage angles of node i at time k, respectively; $V_{i,k}^{\mathrm{true}}$ and θ true i,k are from load flow calculations.

A. Sensitivity Analysis to System Parameter $\mathbf{Q}_k$

We first conduct a sensitivity analysis of the proposed REnKF to the system parameter $\mathbf{Q}_k$. To this end, the probability distribution of $\mathbf{w}_k$ is assumed to be a Gaussian distribution, i.e., $\mathbf{w}_k$: $\boldsymbol{N}(\mathbf{0}, \mathbf{Q}_k)$. On the basis of the prior knowledge, the diagonal elements of $\mathbf{Q}_k$ are set to be constant values in many Kalman filters [8]–[10]. Consequently, the use of relatively small values will yield estimation results predominantly determined by the forecasted states, while the use of relatively large values will provide estimation results that are affected by the real-time measurements. Accordingly, the sensitivity of the proposed method to $\mathbf{Q}_k$ was evaluated based on four representative parameter settings: the time-variant $\mathbf{Q}_k$in (26) with its initial value diag{$\mathbf{Q}_0$} $= 10^{-5}$; the time-variant $\mathbf{Q}_k$ in (26) with its initial value diag{$\mathbf{Q}_0$} $= 10^{-4}$; a constant $\mathbf{Q}$ with diag{$\mathbf{Q}$} $= 10^{-5}$; a constant $\mathbf{Q}$ with diag{$\mathbf{Q}$} $= 10^{-4}$. The MAE values for the predicted and estimated states of all node voltage magnitudes over the 24-h simulation period are shown in Figs. 3 and 4, respectively.

From Fig. 3, we note that the proposed method with large constant $\mathbf{Q}$ obtains the worst results. Meanwhile, the state forecasting model with the time-variant $\mathbf{Q}_k$ maintains a high accuracy despite the value of the initial parameter settings. Similar trends are observed in Fig. 4. As expected, the accuracy of the estimated states is affected by the performance of the state forecasting. Again, we note that the MAE values for the estimated states with the two time-variant $\mathbf{Q}_k$ parameters are nearly the same. These results indicate that the procedure for adjusting $\mathbf{Q}_k$ in the proposed REnKF not only can correct inappropriate parameter settings but also ensure that the forecasting and estimation errors lie within reasonable limits. Accordingly, the time-variant $\mathbf{Q}_k$ with its initial value of diag{$\mathbf{Q}_0$} $= 10^{-5}$ is selected as the system parameter in the following tests.

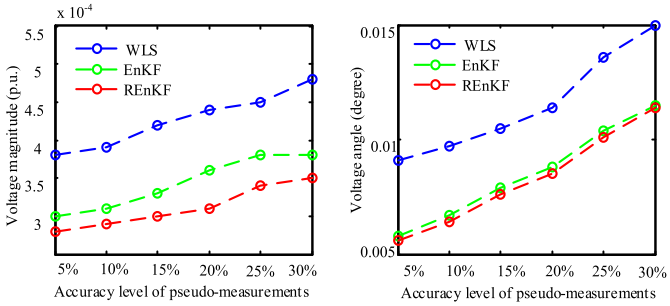

Fig. 5. MAE for estimation results obtained by the different methods with different accuracy levels of pseudomeasurements.

B. Accuracy and Robustness Analysis

To assess the REnKF performance in comparison with other approaches under the same conditions, the MAEs obtained by three methods with different accuracy levels of pseudomeasurements are shown in Fig. 5. As expected, the worse the accuracy level of the pseudomeasurements, the larger are the MAE estimation results. In addition, it is found that the REnKF performs better than EnKF and WLS with the same level of pseudomeasurements accuracy. This is due to the adaptive updating of system process noise covariance matrix in the REnKF. These results also point at the importance of using derived power measurements from smart meters for SE performance improvement.

Furthermore, two different scenarios of erroneous measurements are considered to test the robustness of each method, including: 1) the active and reactive load power measurements at the LV side of node 11 are multiplied by −10 during the 40th to 45th time instants and 2) the power flow measurements at branch 1-2 are multiplied by 3 during the 40th–45th

TABLE I

COMPARISON RESULTS OBTAINED BY DIFFERENT METHODS WITH ERRONEOUS MEASUREMENT IN SCENARIO 1

	Traditional WLS+NR	Traditional EnKF	REnKF +pseudo	Proposed REnKF
MAE of voltage magnitude (p.u.)	4.7×10^{-4}	3.8×10^{-4}	3.5×10^{-4}	2.9×10^{-4}
MAE of voltage angle (degree)	0.0159	0.0119	0.0115	0.0060

TABLE II

COMPARISON RESULTS OBTAINED BY DIFFERENT METHODS WITH ERRONEOUS MEASUREMENT IN SCENARIO 2

	Traditional WLS+NR	Traditional EnKF	REnKF +pseudo	Proposed REnKF
MAE of voltage magnitude (p.u.)	0.0011	0.0010	4.5×10^{-4}	2.8×10^{-4}
MAE of voltage angle (degree)	0.1061	0.1007	0.0194	0.0065

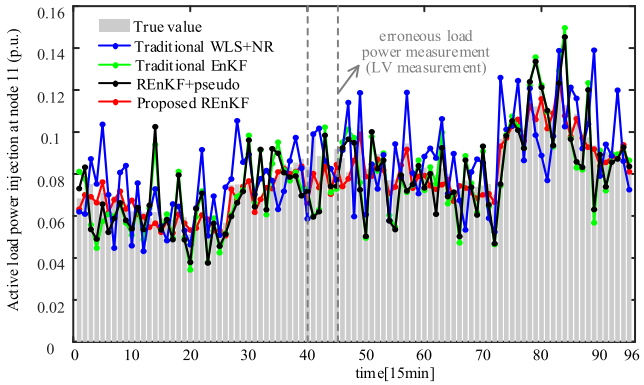

Fig. 6. Estimated values of power consumption at node 11 obtained by the WLS + NR (blue line), the traditional EnKF (green), the REnKF with pseudomeasurements (black), and the proposed REnKF with smart meters (red).

time instants. For the sake of fairness in the comparison, the proposed REnKF that uses the same measurement set as the traditional WLS, namely, REnKF + pseudo, is tested. The average MAE estimation results of the four methods are presented in Tables I and II. In addition, the estimated active power injections at node 11 and power flow at branch 1-2 are displayed in Figs. 6 and 7 for illustrations.

As shown in Tables I and II, the proposed REnKF is able to effectively detect bad data and suppress their influences thanks to the strategic use of PS and the modification of the measurement error covariance matrix. By contrast, both the WLS and EnKF are sensitive to bad data, yielding biased state estimates. As expected, the proposed REnKF shows better robustness owing to the use of LV measurements when compared with the REnKF using the low-precision pseudomeasurements. It is worth pointing out that in scenario 1, the performance of the WLS, EnKF, and REnKF + pseudomethods are not affected as the incorrect measurements from the considered substation are not leveraged. While in scenario 2, once the online MV

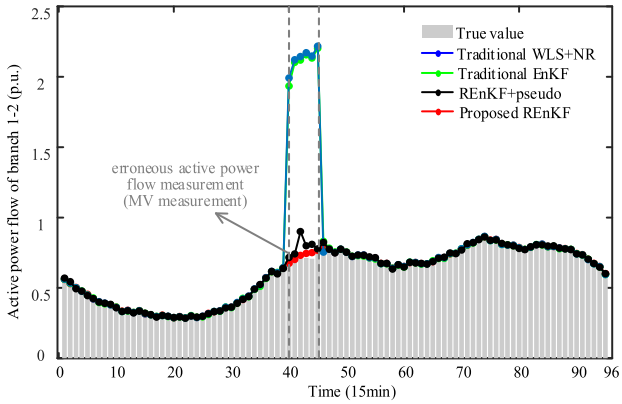

Fig. 7. Estimated values of power flow at branch 1-2 obtained by the traditional WLS + NR (blue line), the traditional EnKF (green), the REnKF with pseudomeasurements (black), and the proposed REnKF with smart meters (red).

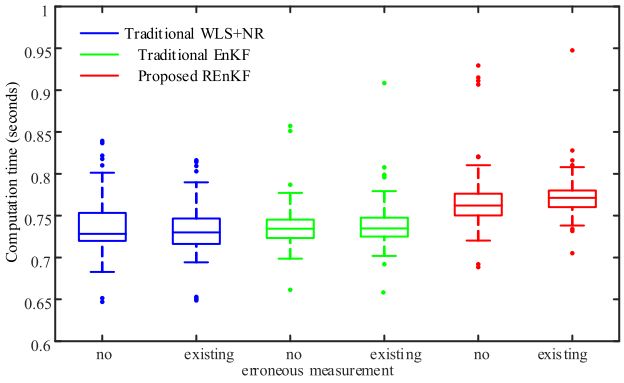

Fig. 8. Computational performance of three methods under two measurement scenarios.

measurements are contaminated, both the WLS and EnKF are unable to handle it. It is interesting that the NR test typically handles well noninteracting and nonconforming bad data given a good level of measurement redundancy. However, this is not the case here as the measurement redundancy for both the WLS and EnKF is low. Furthermore, the pseudomeasurements are with large uncertainties that significantly affect the effectiveness of the NR test. As a result, it can be seen from Fig. 7 that although WLS is used together with the NR test, the bad data are not detected effectively. The REnKF + pseudo proved to perform better than both the WLS and EnKF with the aid of the bad data detection method. Thanks to the enhanced measurement redundancy given by the derived equivalent power measurements from LV smart meters and the use of PS, the proposed REnKF provides the best results and proves that the bad data can be effectively suppressed, yielding only slightly biased estimation results.

C. Computational Performance

The computational performance of each method is assessed in this section. Fig. 8 shows the computing times of the proposed REnKF along with the traditional WLS with NR and the traditional EnKF under the two measurement scenarios. It can be observed from Fig. 8 that the computational efficiency of the traditional WLS with NR and the traditional EnKF are slightly higher than that of the proposed REnKF. The latter

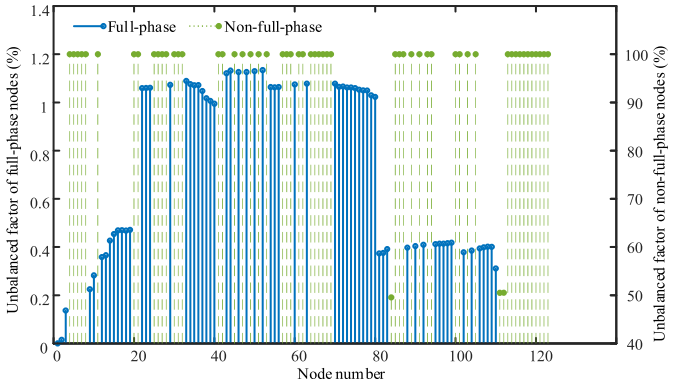

Fig. 9. VUF magnitude for the modified IEEE-123 bus systems.

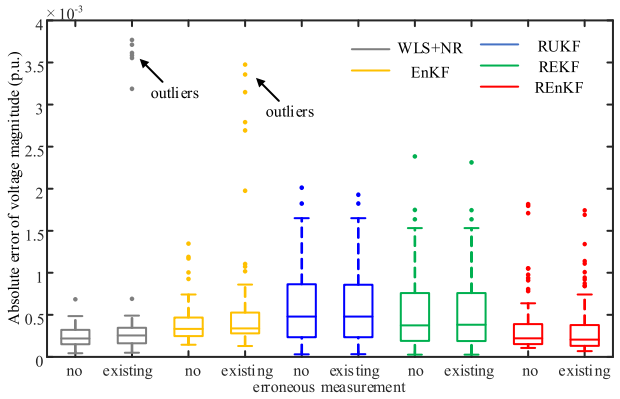

Fig. 10. Estimation results obtained by different methods under two measurement scenarios.

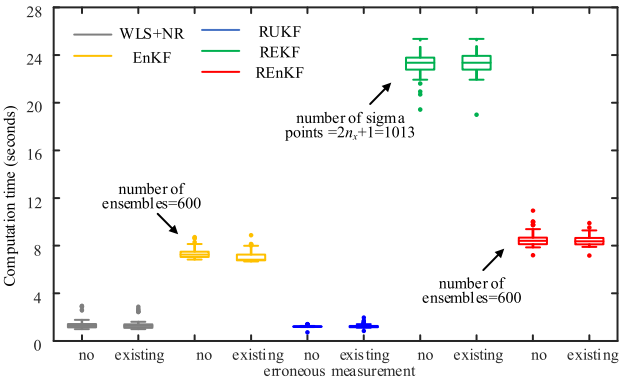

Fig. 11. Computational performance comparison of different methods under two measurement scenarios.

ensures better estimation results and higher robustness at the expense of a small increase in the computation time. It is also shown that the proposed REnKF requires no more than 0.8 s on average to obtain the SE results at each time instant, and the maximum execution time is within 1 s under erroneous measurement scenario. Accordingly, the occurrence of erroneous measurement data has little impact on the computing time. Therefore, if the refresh rate of smart meters becomes faster, i.e., a few minutes, the proposed REnKF can update the system states at a quicker time scale. We would also like to emphasize that the requirement of SE results is different for different applications. For example, 15-min interval for the optimal power flow (OPF) and voltage-var controls may be sufficient while it may not be appropriate for real-time applications. If the distribution system is observable by SCADA measurements with updating rate 2–5 s, the proposed approach can be easily extended to achieve the real-time monitoring capability.

D. Adaptability Analysis Under Unbalanced Conditions

The proposed REnKF is also applied in the modified IEEE 123-bus system with intermittent renewable energy sources, whose data set is available in [35]. A 750-kW wind turbine and a 600-kW solar photovoltaic are connected to bus 96 and bus 33, respectively, as shown in the Appendix. Fig. 9 shows the magnitude of voltage unbalance factor (VUF) [27] for the modified IEEE 123-bus system. It is worth noting that the grid also contains single-phase and two-phase laterals, thus providing a relevant scenario for testing the proposed method under unbalanced conditions. Here, MV measurements are power flow measurements, whose added noise is assumed to be Gaussian with a 1% accuracy level, and the LV measurements include load power injection measurements, whose added noise is assumed to be Gaussian with a 3% accuracy level (as in [32] and [33]). All the measurements used here are from each phase of the modified IEEE 123-bus system. Two different measurement scenarios were considered: 1) no erroneous measurement data and 2) the active and reactive power flow measurements of branch 3-9, at phase A, are multiplied by -3 during the 40th–45th time instants.

As a comparison, four alternative approaches have been tested on the modified IEEE 123-bus system: 1) the traditional WLS + NR; 2) the EnKF; 3) the well-known EKF implemented with the aid of the bad data detection and the model adjustment techniques presented in Section III-B and III-C, called here REKF; and 4) the UKF also implemented with the assistance of the bad data detection and the model adjustment techniques presented in Section III-B and III-C, namely, RUKF. Note that the number of sigma points for the UKF is $2n_x+1$, which is recommended in [7] and [25]. For the sake of a fair comparison, these alternative approaches use the same MV and LV measurement sets as the proposed REnKF. The absolute estimation errors and the computing times over the 24-h simulation period (96 time instants) under two measurement scenarios are, respectively, shown in Figs. 10 and 11.

In Fig. 10, it can be observed that the WLS + NR and the EnKF perform well under the normal measurement condition, but yield significant estimation errors in the presence of erroneous measurements. The other three robust filters, i.e., REKF, RUKF, and REnKF, show stable performance regardless of the presence of erroneous measurements. However, the proposed REnKF still outperforms the REKF and the RUKF. This result thus demonstrates the validity of the proposed REnKF for unbalanced distribution systems with intermittent renewable energy sources. As for the computing time of each approach (see Fig. 11), it inevitably increases when the size of the distribution grid grows, thus leading to larger execution times with respect to the results shown in Section IV-C. It is worth noting that the computational performance of the RUKF and

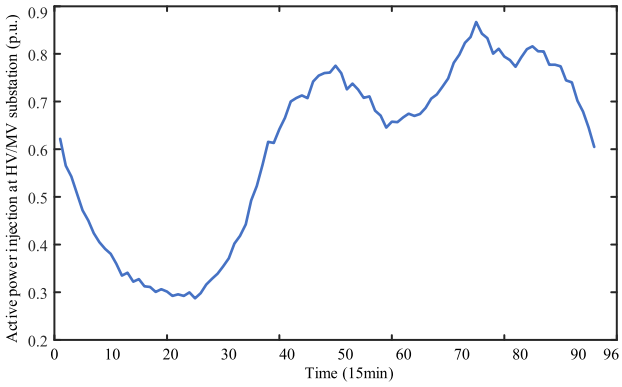

Fig. 12. Active power flow injection at the HV/MV station.

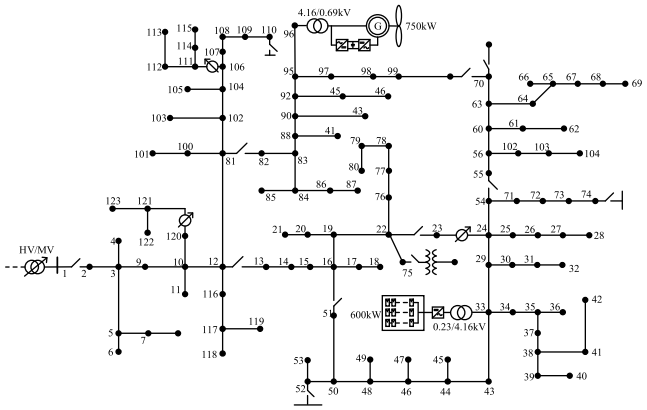

Fig. 13. Topology of the modified 123-bus system.

REnKF are, respectively, affected by the number of sigma points and ensembles. Although the number of sigma points is larger than that of the ensembles, the estimation accuracy of the RUKF is lower than that of the proposed REnKF (see Figs. 10 and 11). Therefore, it could be concluded that the proposed REnKF has better performance than the RUKF in terms of estimation accuracy and computational efficiency. At the same time, it is possible to observe that the computing time of the proposed REnKF is larger than that of the WLS + NR and REKF, but it is still within 11 s. This is acceptable as the SE for distribution systems is typically updated every few minutes. For very large-scale distribution systems, a distributed implementation or the use of parallel computing techniques can be useful to further decrease the computation time and to allow achieving the real-time monitoring of the grid. This is a research direction that we plan to pursue in the near future.

V. Conclusion

In this article, a robust forecasting-aided MV distribution system SE method based on REnKF is proposed. To improve the measurement redundancy, the LV measurements obtained from smart meter devices are used together with the mathematical model of MV/LV substation to derive new equivalent MV measurements. These equivalent measurements have higher precision than the widely used pseudomeasurements, yielding the improvement of estimation accuracy. The temporal correlation-based innovation matrix is developed to allow the detection of bad data via PS. The system process noise covariance matrix is updated adaptively to mitigate the impacts of uncertainties ON-state forecasting and state filtering. Extensive comparisons carried out on an actual and a benchmark test system show that our proposed REnKF is able to obtain accurate SE results under various operation conditions, such as the presence of bad data, unknown noise statistics, and system unbalance.

Appendix

The parameters of the actual MV distribution system shown in Fig. 2 are provided in Tables III and IV. The rated voltage and apparent power are 12.66 kV and 10 MV, respectively. Fig. 12 shows the daily variation of total power flow injected in the feeder by the HV/MV station, and the topology of the modified 123-bus system is shown in Fig. 13.

TABLE III
MV/LV Substation Parameters of Actual MV Distribution System

Node	Rated apparent power (kVA)	P_{no} (kW)	P_{short} (kW)
9,11,16	200	0.8	2.6
5,17	250	0.76	3.25
4,19	315	0.9	4.2
6,7,10,15	630	1.5	7.08
8,12,14,18	1250	2.8	12.5

TABLE IV
Lien Parameters of Actual MV Distribution System

Start node	End node	Resistance (in p.u.)	Reactance (in p.u.)
1	2	0.000926	0.001799
2	3	0.004616	0.010815
3	4	0.000856	0.000874
4	5	0.001284	0.00131
5	6	0.00214	0.00218
6	7	0.00224	0.00198
7	8	0.00194	0.001285
8	9	0.00214	0.001587
9	10	0.00344	0.003184
9	11	0.00274	0.002284
11	12	0.00244	0.00217
3	13	0.006649	0.010033
13	14	0.00214	0.002184
14	15	0.002354	0.002402
15	16	0.002754	0.002502
16	17	0.002854	0.002202
17	18	0.003154	0.0024
13	19	0.004155	0.00627
19	20	0.001662	0.002508

References

[1] R. A. Jabr and I. Džafić, "Sensitivity-based discrete coordinate-descent for Volt/VAr control in distribution networks," *IEEE Trans. Power Syst.*, vol. 31, no. 6, pp. 4670–4678, Nov. 2016.

[2] W. Gu, G. Lou, W. Tan, and X. Yuan, "A nonlinear state estimator-based decentralized secondary voltage control scheme for autonomous microgrids," *IEEE Trans. Power Syst.*, vol. 32, no. 6, pp. 4794–4804, Nov. 2017.

[3] B. P. Hayes and M. Prodanovic, "State forecasting and operational planning for distribution network energy management systems," *IEEE Trans. Smart Grid*, vol. 7, no. 2, pp. 1002–1011, Mar. 2016.

[4] A. Abur and A. G. Exposito, *Power System State Estimation: Theory and Implementation*. New York, NY, USA: Marcel Dekker, 2004.

[5] K. Dehghanpour, Z. Wang, J. Wang, Y. Yuan, and F. Bu, "A survey on state estimation techniques and challenges in smart distribution systems," *IEEE Trans. Smart Grid*, vol. 10, no. 2, pp. 2312–2322, Mar. 2019.

[6] E. Manitsas, R. Singh, B. C. Pal, and G. Strbac, "Distribution system state estimation using an artificial neural network approach for pseudo measurement modeling," *IEEE Trans. Power Syst.*, vol. 27, no. 4, pp. 1888–1896, Nov. 2012.

[7] M. Huang, Z. Wei, G. Sun, Y. Sun, H. Zang, and K. W. Cheung, "A historical data-driven unscented Kalman filter for distribution system state estimation," in *Proc. IEEE Power Energy Soc. Gen. Meeting*, Jul. 2017, pp. 1–5.

[8] S. M. O. Alhalali and R. A. Elshatshat, "State estimator for electrical distribution systems based on a particle filter," in *Proc. IEEE Power Energy Soc. Gen. Meeting*, Jul. 2015, pp. 1–5.

[9] A. M. Kettner and M. Paolone, "Sequential discrete Kalman filter for real-time state estimation in power distribution systems: Theory and implementation," *IEEE Trans. Instrum. Meas.*, vol. 66, no. 9, pp. 2358–2370, Sep. 2017.

[10] C. Carquex, C. Rosenberg, and K. Bhattacharya, "State estimation in power distribution systems based on ensemble Kalman filtering," *IEEE Trans. Power Syst.*, vol. 33, no. 6, pp. 6600–6610, Nov. 2018.

[11] A. Cataliotti, V. Cosentino, D. Di Cara, P. Russotto, E. Telaretti, and G. Tiné, "An innovative measurement approach for load flow analysis in MV smart grids," *IEEE Trans. Smart Grid*, vol. 7, no. 2, pp. 889–896, Mar. 2016.

[12] T. J. Morrell, V. Venkataramanan, A. Srivastava, A. Bose, and C.-C. Liu, "Modeling of electric distribution feeder using smart meter data," in *Proc. IEEE/PES Transmiss. Distrib. Conf. Expo.*, Apr. 2018, pp. 1–9.

[13] I. Džafic, R. A. Jabr, I. Huseinagic, and B. C. Pal, "Multi-phase state estimation featuring industrial-grade distribution network models," *IEEE Trans. Smart Grid*, vol. 8, no. 2, pp. 609–618, Mar. 2017.

[14] J. Peppanen, M. J. Reno, M. Thakkar, S. Grijalva, and R. G. Harley, "Leveraging AMI data for distribution system model calibration and situational awareness," *IEEE Trans. Smart Grid*, vol. 6, no. 4, pp. 2050–2059, Jul. 2015.

[15] M. Sun, Y. Wang, G. Strbac, and C. Kang, "Probabilistic peak load estimation in smart cities using smart meter data," *IEEE Trans. Ind. Electron.*, vol. 66, no. 2, pp. 1608–1618, Feb. 2019.

[16] C. Muscas, M. Pau, P. A. Pegoraro, and S. Sulis, "Uncertainty of voltage profile in PMU-based distribution system state estimation," *IEEE Trans. Instrum. Meas.*, vol. 65, no. 5, pp. 988–998, May 2016.

[17] M. Richter, M. Wolter, A. Naumann, and P. Komarnicki, "Practical experiences on PMU-based linear state estimation in distribution grids," in *Proc. IEEE Power Energy Soc. Gen. Meeting*, Jul. 2016, pp. 1–5.

[18] S. S. S. R. Depuru, L. Wang, V. Devabhaktuni, and N. Gudi, "Smart meters for power grid—Challenges, issues, advantages and status," in *Proc. IEEE/PES Power Syst. Conf. Expo.*, Mar. 2011, pp. 1–7.

[19] A. Al-Wakeel, J. Wu, and N. Jenkins, "State estimation of medium voltage distribution networks using smart meter measurements," *Appl. Energy*, vol. 184, pp. 207–218, Dec. 2016.

[20] Q. Chen, D. Kaleshi, Z. Fan, and S. Armour, "Impact of smart metering data aggregation on distribution system state estimation," *IEEE Trans. Ind. Informat.*, vol. 12, no. 4, pp. 1426–1437, Aug. 2016.

[21] Y. Liao, Y. Weng, G. Liu, and R. Rajagopal, "Urban MV and LV distribution grid topology estimation via group lasso," *IEEE Trans. Power Syst.*, vol. 34, no. 1, pp. 12–27, Jan. 2019.

[22] A. Cataliotti *et al.*, "An improved load flow method for MV networks based on LV load measurements and estimations," *IEEE Trans. Instrum. Meas.*, vol. 68, no. 2, pp. 430–438, Feb. 2019.

[23] T.-H. Chen, M.-S. Chen, T. Inoue, P. Kotas, and E. A. Chebli, "Three-phase cogenerator and transformer models for distribution system analysis," *IEEE Trans. Power Del.*, vol. 6, no. 4, pp. 1671–1681, Oct. 1991.

[24] J. Zhao, M. Netto, and L. Mili, "A robust iterated extended Kalman filter for power system dynamic state estimation," *IEEE Trans. Power Syst.*, vol. 32, no. 4, pp. 3205–3216, Jul. 2017.

[25] J. Zhao and L. Mili, "Robust unscented Kalman filter for power system dynamic state estimation with unknown noise statistics," *IEEE Trans. Smart Grid*, vol. 10, no. 2, pp. 1215–1224, Mar. 2019.

[26] G. Evensen, "The ensemble Kalman filter: Theoretical formulation and practical implementation," *Ocean Dyn.*, vol. 53, no. 4, pp. 343–367, Nov. 2003.

[27] N. C. Woolley and J. V. Milanovic, "Statistical estimation of the source and level of voltage unbalance in distribution networks," *IEEE Trans. Power Del.*, vol. 27, no. 3, pp. 1450–1460, Jul. 2012.

[28] L. Mili, M. G. Cheniae, N. S. Vichare, and P. J. Rousseeuw, "Robust state estimation based on projection statistics [of power systems]," *IEEE Trans. Power Syst.*, vol. 11, no. 2, pp. 1118–1127, May 1996.

[29] K. Myers and B. D. Tapley, "Adaptive sequential estimation with unknown noise statistics," *IEEE Trans. Autom. Control*, vol. 21, no. 4, pp. 520–523, Aug. 1976.

[30] *IEEE Standard Profile for Use of IEEE 1588 Precision Time Protocol in Power System Applications*, IEEE Stardard C37.238-2017 (Revision of IEEE Std C37.238-2011), Jun. 2017, pp. 1–42.

[31] A. Alimardani, F. Therrien, D. Atanackovic, J. Jatskevich, and E. Vaahedi, "Distribution system state estimation based on nonsynchronized smart meters," *IEEE Trans. Smart Grid*, vol. 6, no. 6, pp. 2919–2928, Jun. 2015.

[32] C. Muscas, F. Pilo, G. Pisano, and S. Sulis, "Optimal allocation of multichannel measurement devices for distribution state estimation," *IEEE Trans. Instrum. Meas.*, vol. 58, no. 6, pp. 1929–1937, Jun. 2009.

[33] M. Huang, Z. Wei, M. Pau, F. Ponci, and G. Sun, "Interval state estimation for low-voltage distribution systems based on smart meter data," *IEEE Trans. Instrum. Meas.*, vol. 68, no. 9, pp. 3090–3099, Sep. 2019.

[34] S.-C. Huang, C.-N. Lu, and Y.-L. Lo, "Evaluation of AMI and SCADA data synergy for distribution feeder modeling," *IEEE Trans. Smart Grid*, vol. 6, no. 4, pp. 1639–1647, Jul. 2015.

[35] *IEEE PES AMPS DSAS Test Feeder Working Group*. Accessed: Apr. 2019. [Online]. Available: http://sites.ieee.org/pes-testfeeders/resources/

Manyun Huang (S'15) received the B.S. degree from the College of Energy and Electrical Engineering, Hohai University, Nanjing, China, in 2014, where she is currently pursuing the Ph.D. degree.

From September 2017 to September 2018, she was a joint Ph.D. Student with RWTH Aachen University, Aachen, Germany. Her current research interests include the theory and algorithms of power system state estimation, robust state estimation, and Kalman filter.

Zhinong Wei (M'14) received the B.S. degree from the Hefei University of Technology, Hefei, China, in 1984, the M.S. degree from Southeast University, Nanjing, China, in 1987, and the Ph.D. degree from Hohai University, Nanjing, in 2004.

He is currently a Professor of electrical engineering with the College of Energy and Electrical Engineering, Hohai University. His current research interests include power system state estimation, integrated energy systems, smart distribution systems, optimization and planning, load forecasting, and integration of distributed generation into electric power systems.

Junbo Zhao (M'18) received the Ph.D. degree from the Bradley Department of Electrical and Computer Engineering, Virginia Tech, Blacksburg, VA, USA, in 2018.

He was an Assistant Professor (Research) with Virginia Tech from May 2018 to August 2019. He is currently an Assistant Professor with Mississippi State University, Starkville, MS, USA. His current research interests include power system modeling, real-time monitoring, dynamics and cyber security that include state estimation, dynamics and stability, cyber-attacks and countermeasures, big data analytics, and robust statistics with applications in the smart grid.

Dr. Zhao was a co-receipient of the Best Paper Award of the 2019 IEEE PES ISGT Asia. He was the best Reviewer for the IEEE TRANSACTIONS ON POWER SYSTEMS 2018. He serves as the Associate Editor for the *International Journal of Electrical Power & Energy Systems* and the *CSEE Journal of Power and Energy Systems*, and the Subject Editor of the *IET Generation, Transmission & Distribution*.

Rabih A. Jabr (M'02–SM'09–F'16) was born in Lebanon. He received the B.E. degree (Hons.) in electrical engineering from the American University of Beirut, Beirut, Lebanon, in 1997, and the Ph.D. degree in electrical engineering from Imperial College London, London, U.K., in 2000.

He is currently a Professor with the Department of Electrical and Computer Engineering, American University of Beirut. His current research interests include mathematical optimization techniques and power system analysis and computing.

Marco Pau (S'14–M'15) received the M.S. degree *(cum laude)* in electrical engineering and the Ph.D. degree in electronic engineering and computer science from the University of Cagliari, Cagliari, Italy, in 2011 and 2015, respectively.

He is currently a Research Associate with the Institute for Automation of Complex Power Systems, E.ON Energy Research Center, RWTH Aachen University, Aachen, Germany, where he is the Leader of the team for Power System Automation. His current research interests include the design of measurement systems applied to electric distribution systems and devised for distribution grid automation.

Guoqiang Sun (M'14) received the B.S., M.S., and Ph.D. degrees in electrical engineering from Hohai University, Nanjing, China, in 2001, 2005, and 2010, respectively.

He was a Visiting Scholar with North Carolina State University, Raleigh, NC, USA, from 2015 to 2016. He is currently an Associate Professor with the College of Energy and Electrical Engineering, Hohai University. His current research interests include power system analysis and economic dispatch and optimal control of integrated energy systems.